Nature of Sodium Atoms/(Na^+, e^-) Contact Pairs in Liquid Tetrahydrofuran

William J. Glover,[†] Ross E. Larsen,[‡] and Benjamin J. Schwartz*

Department of Chemistry and Biochemistry, University of California, Los Angeles, Los Angeles, California 90095-1569

Received: April 30, 2010; Revised Manuscript Received: July 1, 2010

With no internal vibrational or rotational degrees of freedom, atomic solutes serve as the simplest possible probe of a condensed-phase environment's influence on solute electronic structure. Of the various atomic species that can be formed in solution, the quasi-one-electron alkali atoms in ether solvents have been the most widely studied experimentally, primarily due to the convenient location of their absorption spectra at visible wavelengths. The nature of solvated alkali atoms, however, remains controversial: the consensus view is that solvated alkali atoms exist as (Na^+, e^-) tight-contact pairs (TCPs), species in which the alkali valence electron is significantly displaced from the alkali nucleus and confined primarily by the first solvent shell. Thus, to shed light on the nature of alkali atoms in solution and to further our understanding of condensed-phase effects on solutes' electronic structure, we have performed mixed quantum/classical molecular dynamics simulations of sodium atoms in liquid tetrahydrofuran (Na^0/THF). Our interest in this particular system stems from recent pump−probe experiments in our group, which found that the rate at which this species is solvated depends on how it was created (*Science* **2008**, *321*, 1817); in other words, the solvation dynamics of this system do not obey linear response. Our simulations reproduce the experimental spectroscopy of this system and clearly indicate that neutral Na atoms exist as (Na^+, e^-) TCPs in solution. We find that the driving force for the displacement of sodium's valence electron is the formation of a tight solvation shell around the partially exposed Na^+. On average, four THF oxygens coordinate the cation end of the TCP; however, we also observe fluctuations to other solvent coordination numbers. Furthermore, we find that species with different solvent coordination numbers have unique absorption spectra and that interconversion between species with different solvent coordination numbers requires surmounting a free energy barrier of several k_BT. Taken together, our results suggest that the Na^0/THF species with different solvent coordination numbers may be viewed as chemically distinct. Thus, we can explain the kinetics of Na TCP formation as being dictated by changes in the Na^+ solvent coordination number, and we can understand the dependence on initial conditions seen in the solvation dynamics of this system as resulting from the fact that the important solvent coordinate involves the motion of only a few molecules in the first solvation shell.

1. Introduction

Solvents not only provide a medium in which chemical species can meet and react but also provide an environment that can modify the electronic structure of dissolved molecules, which in turn can dramatically alter solution-phase reactivity relative to that in the gas phase. Knowing how a condensed-phase environment affects the electronic structure of solutes is therefore crucial for a detailed understanding of solution-phase chemistry. The simplest type of solute with which to probe such condensed-phase effects is an atom: atoms have only translational and electronic degrees of freedom, so any solvent-induced effects on their electronic structure are easy to quantify, particularly in comparison to molecular solutes whose conformational degrees of freedom also can be altered by solvent interactions.

Unfortunately, there are relatively few substances that will dissolve atomically in liquids, and the few that do have electronic absorption spectra that are located at wavelengths where it is not experimentally convenient to probe the effects of a condensed-phase environment. Notable exceptions are the alkali metal atoms, which can be formed transiently in liquid ether solvents through the reaction of solvated electrons with alkali cations, as is commonly performed in pulse radiolysis experiments.[1,2] There has been some debate, however, about how to think of the electronic structure of the quasi-one-electron alkalis when they are dissolved in liquids. Many workers have argued that neutral alkali atoms in ether solvents exist as tight-contact pairs (TCPs), species that are better written as (M^+, e^-) because the electron is significantly displaced from the M^+ cation so that the identity of the atom is strongly perturbed from that in the gas phase.[1−4] This interpretation is supported by electron spin resonance (ESR) measurements, which found that the valence electron of K^0 in liquid tetrahydrofuran (THF) has only ∼36% atomic character,[5] suggesting that K^0/THF has an identity somewhere between that of a solvated neutral atom and a separated solvated electron/K^+ ion pair. This idea is also supported by the fact that the absorption spectra of neutral alkali atoms in ethers are broad and have maxima between those of the gas-phase alkali atom D-lines and the solvated electron. For example, the absorption spectrum of (Na^+, e^-) in liquid THF peaks at around 1.4 eV,[4] roughly halfway between the isolated Na^0 D-line at 2.1 eV and the absorption maximum of the THF-

* To whom correspondence should be addressed: E-mail: schwartz@chem.ucla.edu.
[†] Current address: Department of Chemistry, Stanford University, Stanford, CA 94305-5080.
[‡] Current address: National Renewable Energy Laboratory, Golden, CO 80401-3305.

10.1021/jp103961j
Published on Web 08/12/2010

solvated electron at 0.59 eV.[6] There is no direct experimental proof, however, that alkali atoms exist as TCPs in ether solvents; an alternative picture is that the atom's valence electron remains centered on the nucleus but is diffusely distributed over many solvent molecules, weakening the overlap with the alkali metal core.[7]

The question of how a single alkali atom behaves in solution-phase environments has been explored to a limited extent by simulation. For example, Sprik et al. studied the properties of Li^0 in liquid ammonia using path-integral Monte Carlo simulations, and found that Li^0 exists as a tight-contact pair with two ammonia molecules solvating the Li^+ through the nitrogen atoms.[8] However, more recent work suggests that this species is not present in Li/NH_3 solutions.[9,10] Building on previous work,[11] Coudert et al. have explored the properties of electron-alkali cation contact pairs in liquid water using mixed quantum/classical molecular dynamics (MQC MD) simulations.[12] From free energy calculations, they found that the dissociated alkali atoms were no more than a few k_BT higher in energy than a tight-contact pair, with a barrier of less than 10 k_BT separating these species. This implies that aqueous solutions of alkali cations and hydrated electrons should exhibit a statistical distribution of species rather than specifically forming contact pairs.[12] This previous work is suggestive, but to the best of our knowledge, there has been no simulation work targeted at experimentally realizable alkali cation-electron tight-contact pairs, such as the alkali atoms in liquid ethers.

To better understand the nature of solvated alkali atoms that are not largely dissociated, in this paper we present the results of MQC MD simulations of Na^0/THF. We chose this particular solute/solvent combination as it is the most studied experimentally,[1−4,13−17] providing the best possibilities for confronting theory with experiment. Our preliminary simulation studies of this system found that Na^0 clearly exists as a TCP in liquid THF,[18] in agreement with experimental interpretations.[1−4,13−15,19] In this work, we explore the molecular nature of the sodium TCP in significantly more detail. We find that the driving force for TCP formation lies in the creation of a tight solvation shell of ∼4 THF oxygens around the partially exposed Na^+ end of the TCP. We also find that the number of solvent oxygen sites coordinating the cation end of (Na^+, e^-)/THF fluctuates, and that changing the coordination number requires surmounting a barrier of a few k_BT. Moreover, we see that TCP species with different solvent coordination numbers have unique electronic absorption spectra, which shift from the visible (gas-phase Na^0-like) to the near-IR (solvated electron-like) with increasing solvent coordination. Thus, (Na^+, e^-)/THF species with different cation solvent coordination numbers can be thought of as chemically distinct. We also note that the Na^0/THF species was the highlight of recent pump−probe experiments in our laboratory that suggested a breakdown of the linear response (LR) approximation for the solvation dynamics of this system.[15] Our simulations now allow us to understand the solvation dynamics of Na^0/THF as being dominated by changes in the number of solvent oxygen sites coordinating the Na^+, explaining the apparent failure of LR.

2. Methods: Mixed Quantum/Classical Molecular Dynamics

We simulated Na^0/THF using mixed quantum/classical molecular dynamics (MQC MD) simulations in which the 3s valence electron of Na was treated quantum mechanically and all other particles (Na^+ core and solvent) were treated classically. Our methodology is similar to one-electron models that have been used previously to study the electronic properties of alkali atoms in a variety of clusters and condensed-phase environments.[8,9,11,20−23] Our simulated system consisted of 255 classical tetrahydrofuran (THF) solvent molecules, one classical Na^+ solute core, and one quantum-mechanical electron. The details of the classical model that we used have been presented elsewhere.[24] Briefly, the THF molecules were treated as rigid, planar five-membered rings with classical interaction potentials that were taken from the optimized potentials for liquid simulations model.[25,26] The interactions between the classical particles and the quantum-mechanically treated electron were accounted for using Philips−Kleinman (PK) pseudopotentials[27] that we previously developed for both sodium[28] and THF.[29,30] To correct for the frozen-core approximation in the PK formalism, the pseudopotentials were augmented with polarization potentials that have been described elsewhere.[30] Periodic boundary conditions were implemented with the minimum image convention[31] and all interactions were tapered smoothly to zero at 16 Å over a 2 Å range with a center-of-mass-based Steinhauser switching function.[32] We verified that truncating intermolecular interactions in this way did not introduce any artifacts by comparing the solvent structure of Na^+ in THF simulated with our code to the solvent structure of a simulation using identical potentials in the Gromacs software package[33] that treated the long-range interactions using the particle mesh Ewald method.

For the quantum mechanical electron, the electronic eigenstates were expanded in a basis of 32 × 32 × 32 plane waves that spanned the cubic simulation cell and the single-electron Hamiltonian was diagonalized at every MD time step using the implicitly restarted Lanczos method[34] as implemented in ARPACK.[35] The MD trajectory was propagated adiabatically on the electronic ground-state surface using the velocity Verlet algorithm[31] with a 4 fs time step.[36] The THF molecules were held rigid and planar with the RATTLE algorithm,[38] as described in more detail in the Supporting Information. Our simulations were performed in the canonical ensemble, with particle velocities coupled to Bussi's stochastic thermostat.[39] The average temperature was set to 298 K with a thermostat relaxation time of 0.5 ps. The simulation cell length was fixed at 32.50 Å, corresponding to the experimental density of pure liquid THF, $\rho = 0.8892$ g cm^{-3}.[37]

We initiated a 1 ns simulation trajectory by adding a quantum mechanical electron in its electronic ground state to an equilibrated classical simulation of Na^+ in THF; we then re-equilibrated the resulting MQC system for 50 ps. We found that the electron initially was delocalized over much of the simulation cell, but that within a few picoseconds it attached to the Na^+ to form the TCP species. To reduce the computational expense, we calculated only the electronic ground state at each MD time step, as necessary to propagate the adiabatic MQC dynamics. To obtain spectra from our simulations, we also calculated 19 excited states using single-point calculations on snapshots extracted from the MD trajectory that were separated by 100 fs.

3. Results and Discussion

3.1. Nature of the Neutral Sodium Species in THF. To determine how well our simulation model can reproduce experiment, we begin our discussion of the nature of the neutral sodium species in THF by calculating its electronic absorption spectrum, $I(E)$, in the inhomogeneous broadening limit:

$$I(E) \propto \langle \sum_j |\boldsymbol{\mu}_{0j}|^2 \Delta E_{0j} \delta(E - \Delta E_{0j}) \rangle \quad (1)$$

where ΔE_{0j} and $\boldsymbol{\mu}_{0j}$ are the energy gap and the transition dipole moments between the ground and jth excited state, respectively. Using the lowest 20 adiabatic states, we evaluated eq 1 every 100 fs from the 1 ns trajectory and then histogrammed the results using 0.1 eV bin widths. The spectrum of Na^0/THF obtained this way is plotted as the solid black curve in Figure 1; the dashed black curve shows the Gaussian−Lorentzian fit to the experimental absorption spectrum.[4] Although there is a slight blue shift of the peak and an underestimate of the blue tail, the figure shows that our calculated spectrum is well within the typical accuracy of one-electron MQC models.[40−43] We thus consider the simulated spectrum as having a good agreement with experiment, giving us confidence that our simulation model faithfully captures the essential electronic properties of Na^0/THF.

To understand the origins of the spectrum, the colored curves in Figure 1 show contributions to the total spectrum from transitions to the four lowest adiabatic excited states; clearly, the lowest three excited states have the largest contribution to the absorption spectrum, and the higher-lying states make up the blue spectral tail. Inspection of the excited electronic wave functions reveals that the lowest three excited states correspond to p-like orbitals; these orbitals occur at an energy lower than that in the gas phase; thus, the solution environment has decreased the gas-phase 3s−3p gap of 2.14 eV for Na^0 (in our model[28]) to the observed peak at ∼1.65 eV (1.43 eV experimental[4]) in the Na^0/THF absorption spectrum. We also see that the width in the simulated absorption spectrum results both from a splitting of ∼0.4 eV between the highest and lowest p-like states and from the full width at half-maximum (fwhm) of ∼0.4 eV of each subband. The resulting total simulated absorption spectrum has a fwhm of ∼0.65 eV, which is somewhat narrower than the experimental fwhm of 0.849 eV.[4] The fact that the spectral width in our calculations is smaller than experiment appears to be a consequence of underestimating the blue tail of the spectrum, which likely results from the fact that we included only the lowest 19 electronic excited states when calculating the spectrum or possibly from factors discussed in ref 42.

The large splitting between the lowest p-like excited states of Na^0/THF (which are degenerate in the gas phase) is indicative of a considerable asymmetry in the local solvent environment around Na^0. To better understand this asymmetry in the local solvation structure, we show a representative MD snapshot of Na^0/THF in Figure 2. For clarity, we show only the THF molecules in the first solvation shell (represented as licorice bonds), defined as those whose centers-of-mass (COM) were within 5.6 Å of the electron COM; this distance corresponds to the location of the minimum in the THF-COM: e^-−COM radial distribution function (see Figure 3, below). In the Figure 2 snapshot, the sodium cation is plotted as a black sphere with the Na^+ ionic radius, and the electron is shown as a translucent blue surface enclosing 50% of the valence charge density. Clearly, the electron density is substantially displaced from the sodium cation, giving an average dipole moment of 1.43 ± 0.04 e Å (6.87 D). We also see that although the electron is displaced, it still occupies the same solvent cavity as the Na^+. Our simulations thus identify Na^0/THF as a tight-contact pair at equilibrium, in agreement with experimental interpretations.[1−4] Although the sodium cation-solvated electron TCP is usually written as (Na^+, e^-), for reasons that will become clear below

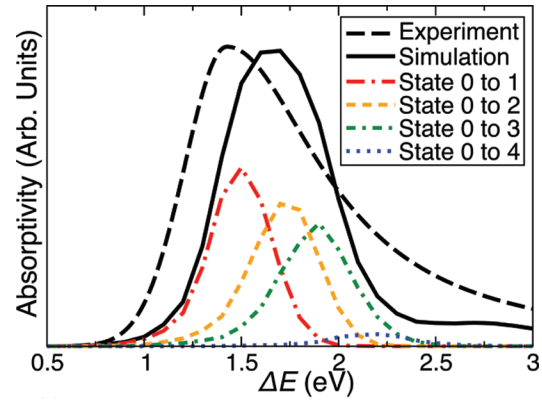

Figure 1. Absorption spectrum of the equilibrium neutral sodium species in THF from simulation (solid black curve) compared to the Gaussian−Lorentzian fit of the experimental absorption spectrum (ref 4, dashed black curve). Also shown are individual contributions to the calculated spectrum from transitions to the lowest four excited states: state 1, red long dash dotted curve; state 2, orange short dashed; state 3, green short dash dotted; state 4, blue dotted.

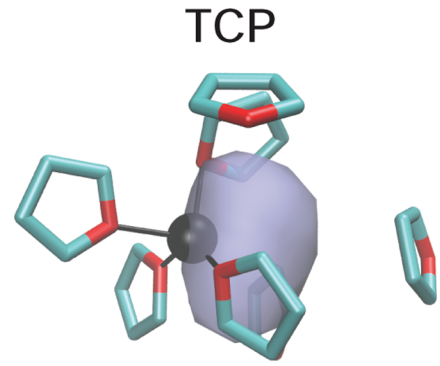

Figure 2. Molecular dynamics snapshot of the equilibrium neutral sodium species in THF. The first solvation shell THF molecules are plotted as licorice, the Na^+ core as a black sphere (scaled to its ionic radius) and the valence electron represented as a translucent blue surface enclosing 50% of the charge density. Bonds are drawn between Na^+ and THF oxygen sites within 3.65 Å. Clearly the neutral sodium species is a tight-contact pair (TCP) and not a solvated atom.

when we explore different coordination numbers around the cation, we shall continue to refer to this species as Na^0.

One of the key features of the solvation structure of Na^0/THF is that displacement of the valence electron exposes the Na^+ core, allowing it to be directly solvated by THF. We find that the Na^+ core is coordinated, on average, by four THF molecules through their negatively charged oxygen sites; these coordinating interactions are shown in Figure 2 as the black bonds between the oxygen sites and the Na^+. Figure 2 also shows that on the electron side of the neutral sodium TCP, the solvent oxygen sites preferentially point away from the electron. This unusual solvation structure around Na^0/THF is explored in more detail in Figure 3, which plots the radial distribution function, $g(r)$, of Na^+−THF oxygen distances. We see that $g(r)$ is dominated by a large peak with a magnitude over 25 (as shown in the inset to Figure 3) at 2.35 Å; this peak corresponds to the THF oxygen sites that solvate the Na^+ end of the TCP. This 2.35 Å peak is at the exact same distance as the first solvation shell peak of THF oxygen sites solvating a bare Na^+ in THF,[25] confirming that the exposed Na^+ side of the TCP is solvated in the same manner whether or not the electron is present. The chief difference the electron makes is in the cation coordination number: a single Na^+ in liquid THF is coordinated by six first-shell THF oxygen sites,[25] whereas for Na^0, integrat-

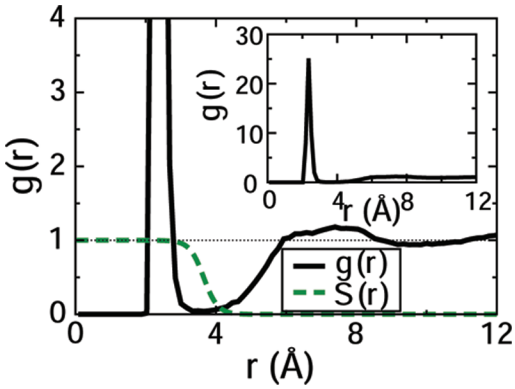

Figure 3. Radial distribution function (RDF), $g(r)$ (solid black curve), for Na^+-THF oxygen site distances for the neutral sodium species in THF. The dashed green curve shows the smooth cutoff function, $S(r)$, used to define the inner solvation shell around Na^+ in eq 2. The inset expands the y-axis scale to better show the large peak in the RDF.

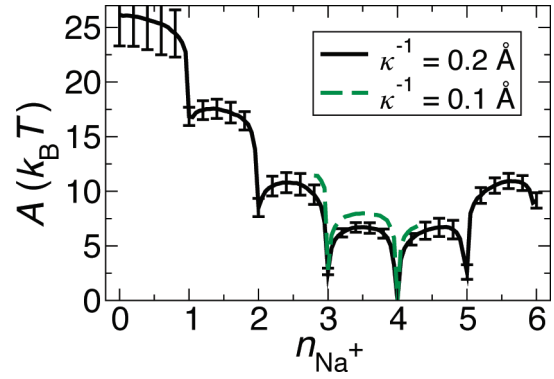

Figure 4. Free energy, A, as a function of the Na^+ coordination number collective variable, n_{Na^+}, for Na^0/THF. A is plotted for two values of κ^{-1}, the transition width of the smooth cutoff function used to define n_{Na^+} (eq 3): $\kappa^{-1} = 0.2$, Å, solid black curve; $\kappa^{-1} = 0.1$ Å, dashed green curve (shown only for $2.8 \leq n_{Na^+} \leq 4.2$). Error bars represent the 95% confidence interval. The integer coordination numbers 1−6 are seen to correspond to free-energy local minima with barriers of a few k_BT separating them.

ing $g(r)$ up to the first minimum at 3.65 Å gives an average coordination number of 3.98: the fact that the electron occupies space near the cation causes the first solvation shell around the Na^+ end of the TCP to be only partially developed.

3.2. Factors Determining the Coordination Number of Na^0/THF. To understand why the four-coordinated species of Na^0/THF is dominant at equilibrium, we calculated the relative free energies of the different possible Na^0 coordination species. To achieve this, we followed the ideas of Sprik[44] and calculated the free energy, A, as a function of a continuous coordination number variable, n_{Na^+}, which is defined as

$$n_{Na^+} = \sum_i S(|r_{O,i} - r_{Na^+}|) \tag{2}$$

where i runs over every THF oxygen site, and r_{Na^+} and $r_{O,i}$ are the positions of the sodium cation core and the ith oxygen site, respectively. In eq 2, $S(r)$ is a Fermi function, defined as

$$S(r) = \frac{1}{\exp[\kappa(r - r_c)] + 1} \tag{3}$$

where r_c is a cutoff radius that defines when a solvent molecule is coordinated to the cation and κ^{-1} is the width of the transition region where the Fermi function switches from 1 to 0 around r_c. Although the Fermi function is never exactly equal to 0 or 1 except in the limits $r \to \pm\infty$, $S(r)$ can be made numerically close to these values away from the cutoff radius by setting κ^{-1} to be significantly smaller than r_c. We chose $r_c = 3.65$ Å to correspond to the first minimum in the Na^+-O radial distribution function, and we chose $\kappa^{-1} = 0.2$ Å by requiring that the ensemble-averaged coordination number be converged to within 0.01 (i.e., $\langle n_{Na^+} \rangle = 3.98 \pm 0.01$). The green dashed curve in Figure 3 shows $S(r)$ with our chosen parameters.

With a continuous coordination number defined, we then performed umbrella sampling (US) to map out the free energy as a function of n_{Na^+}. To do this, we added a (classical) biasing potential to the system's Hamiltonian:

$$V^{bias} = \frac{1}{2}k(n_{Na^+} - \eta)^2 \tag{4}$$

where η is the coordination number to which we desire to bias the system and k is the biasing potential's spring constant, which we set to $k = 1.25$ eV. We ran US trajectories with 26 different biasing potentials using $\eta_i = (2i - 1)/6$ with $i = 1, ..., 19$ (where i is the index of each biasing "window") and $\eta_i = 0.0, 1.0, ..., 6.0$ for the remaining 7 windows. For each biasing potential, we propagated 0.5 ns of MQC dynamics after an initial equilibration period of 10 ps. To reduce the amount of equilibration time, we chose initial particle coordinates and velocities for each window from an equilibrated snapshot of the adjacent window (e.g., the trajectory in the $\eta = 4\ ^1/_6$ window was initialized from the $\eta = 4.0$ window, which itself was initialized from the original unbiased 1-ns equilibrium simulation).

From the distributions of n_{Na^+} in the 26 windows, we generated the free energy $A(n_{Na^+})$ as a function of the coordination number variable using Grossfield's implementation[45] of the weighted histogram averaging method (WHAM);[46] we chose 121 histogram bins centered at $n_{Na^+} = 0.00$ up to $n_{Na^+} = 6.00$ in increments of 0.05.[47,48] We estimated the statistical uncertainty in the free energy by calculating A from five 0.1 ns blocks of data from each window. The solid black curve in Figure 4 shows $A(n_{Na^+})$ in units of k_BT (for our system temperature $T = 298$ K); the error bars represent 95% confidence intervals. This figure confirms that the four-coordinated species is dominant at equilibrium and that coordination numbers 3 and 5 (which are less than 3 k_BT higher in free energy) are readily thermally accessible. Indeed, our unbiased 1 ns simulation showed occasional fluctuations between coordination numbers 3, 4, and 5 with relative populations of roughly 9:84:7 (see Supporting Information). What is perhaps most striking about Figure 4 is that local minima appear in A at the integer values of n_{Na^+}, with barriers of a few k_BT separating each minimum.[49] The existence of these barriers suggests that we should think about Na^0/THF species with different solvent coordination numbers as being chemically distinct, with interconversion between coordination numbers being an activated process. Thus, for the rest of this paper, we will focus on the integer coordination numbers and explore their properties and relative free energies.

To understand the properties of Na^0/THF with different solvent coordination numbers, we calculated the values of various observables according to

$$X_n = \frac{\langle X\delta(n_{Na^+} - n)e^{V^{bias}/k_BT}\rangle_n}{\langle \delta(n_{Na^+} - n)e^{V^{bias}/k_BT}\rangle_n} \quad (5)$$

where X is the observable, n is the coordination number of interest, and $\langle\ \rangle_n$ represents taking an ensemble average over the US window with $\eta = n$ (for the integer-valued windows only). The delta function in eq 5 was treated numerically by binning values of n_{Na^+} near each integer; we chose a bin width of 0.05 to match the histogram bin width used in generating Figure 4.

We begin our analysis by replotting the relative free energies of the Na^0 species with different solvent coordination numbers as the black curve in Figure 5a.[50] To understand why the four-coordinated species is favored, we calculated the internal energy, E (corrected for the biasing potential), for each integer-coordinated species, shown by the red dashed lines in Figure 5a; we chose the arbitrary zero of internal energy to be that of the 4-coordinated species. The figure makes clear that the internal energy of the system monotonically decreases with increasing coordination of the Na^+; in particular, the six-coordinated species is energetically favored over the lower coordination numbers. We also calculated the entropic contribution to the free energy using the definition of the Helmholtz free energy: $A = E - TS$, where S is the entropy (relative to the 4-coordinated species), plotted as the blue dot-dashed lines in Figure 5a. Clearly, $-TS$ increases monotonically with increasing cation solvent coordination, which makes physical sense as one expects an entropic penalty to forming the highly ordered solvation shell around Na^+. The decrease in entropy with coordination number suggests that at lower temperatures, more highly coordinated species will be favored. This agrees with experimental observations: ESR studies found that the average atomic character of the related neutral potassium and rubidium species in THF decreased sharply with decreasing temperature.[51] In addition, pulse radiolysis experiments found that the absorption spectra of alkali metal atoms dissolved in ether solvents shift to that of a loose contact pair as the temperature is lowered,[52,53] as expected for increasing cation coordination (see ref 18 and Figure 7, below). Indeed, as we show in the Supporting Information, preliminary simulations confirm that the neutral sodium species favors higher coordination numbers at low temperature.

We can further examine the chemical nature of the differently coordinated Na^0/THF species by decomposing the internal energy, E, into solute−solvent and solvent−solvent terms:

$$E = E_{Na^+} + E_{e^-} + E_{THF} + E_K \quad (6)$$

where E_{Na^+} is the classical potential energy of the sodium cation (from interactions with the THF solvent), E_{e^-} is the quantum energy of the valence electron, E_{THF} is the classical THF−THF potential energy, and E_K is the classical kinetic energy (whose average is constant in the canonical ensemble, so that E_K has the same value for each species and thus can be ignored). We plot the various potential energy contributions to the internal energy as a function of coordination number in Figure 5b. As expected, E_{Na^+} (green circles) provides the main energetic driving force to higher coordination numbers, with the addition of each coordinating solvent molecule lowering the E_{Na^+} energy by ~1 eV. In contrast, the solvent reorganization energy, E_{THF} (violet diamonds), increases with increasing coordination number; this makes physical sense since the alignment of the THF dipole to favorably solvate Na^+ comes at the expense of an increase in THF−THF potential energy. Similarly, E_{e^-} (orange squares), which is equal to the negative of the vertical ionization energy of the sodium atom relative to vacuum, also counteracts the energetic drive to higher coordination number from solvating the cation, showing a roughly linear increase from $E_{e^-} = -6.74 \pm 0.06$ eV for $n_{Na^+} = 0$ to $E_{e^-} = -3.44 \pm 0.02$ eV for $n_{Na^+} = 6$. This change in electronic energy shows that Na^0 is becoming increasingly (partially) ionized with increasing solvent coordination. Overall, the analysis in Figure 5 indicates that the four-coordinated species is dominant at equilibrium due to a balance in several energetic considerations: high coordination numbers are favored by the solvation energy of Na^+, and low coordination numbers are favored in minimizing the energetic cost of (partially) ionizing Na^0 and minimizing the solvent's energetic and entropic cost of forming an ordered solvent shell around Na^+.

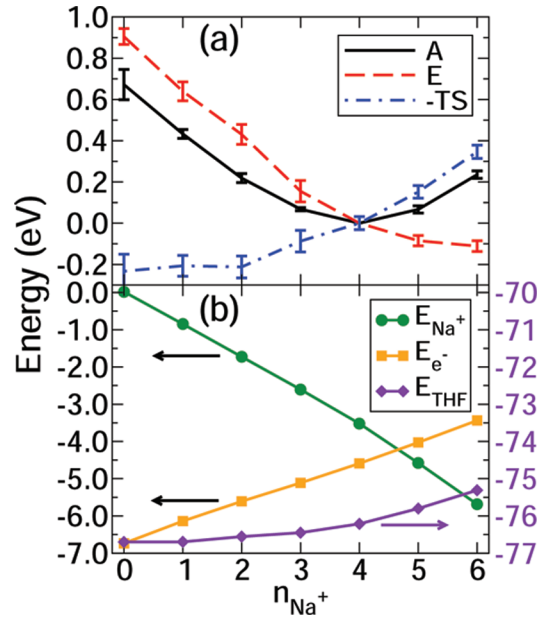

Figure 5. Energetic and entropic contributions to the coordination number free energies, A, of Na^0/THF. Only values at integer coordination numbers are considered, and connecting lines are drawn to guide the eye. (a) shows the decomposition of A (solid black curve) into internal energy, E (red dashed curve), and entropic contributions, $-TS$ (blue dot dashed curve). Coordination number 4 serves as the reference point and the error bars represent 95% confidence intervals. (b) shows the average classical Na^+ potential energy, E_{Na^+} (green circles, left energy axis), the electronic quantum energy, E_{e^-} (orange squares, left energy axis), and the intermolecular THF−THF potential energy, E_{THF} (violet diamonds, right energy axis) relative to vacuum. The error bars in (b) are approximately the size of the symbols and thus are not shown.

3.3. Changes in the Electronic Structure of Na^0/THF with Coordination Number. The fact that the ionization energy of Na^0 changes so dramatically with solvent coordination number suggests that the presence (or absence) of a single coordinating THF solvent molecule can produce large changes in the electronic structure of the neutral atomic sodium species. Some of the other dramatic solvent-induced changes in the electronic structure of Na^0/THF are summarized in Table 1, which shows the average dipole moment, μ, and radius of gyration, $R_{gyr} = \langle\psi|\hat{r}^2|\psi\rangle^{1/2}$, where ψ is the electronic ground state and $\hat{r}$ is the position operator relative to the electron's center of mass, for each solvent coordination number. For reference, the table also includes values for both gas-phase Na^0 and the solvated electron in THF.[30]

TABLE 1: Changes in Na^0 Dipole Moment, μ, and Valence Charge Radius of Gyration, R_{gyr}, with THF Oxygen Site Coordination Number

coord	μ (e Å)	R_{gyr}
gas[a]	0.0	2.302
0	0.18 ± 0.01	2.081 ± 0.005
1	0.51 ± 0.01	2.157 ± 0.004
2	0.83 ± 0.02	2.25 ± 0.01
3	1.11 ± 0.03	2.35 ± 0.01
4	1.44 ± 0.02	2.52 ± 0.01
5	1.96 ± 0.07	2.83 ± 0.02
6	2.70 ± 0.02	3.49 ± 0.02
(e_{THF}^-)[b]		4.49 ± 0.04

[a] Properties of an isolated gas-phase Na^0 atom from our MQC model. [b] Properties of a solvated electron in THF from our MQC model (see ref 30).

The near-zero value of the dipole moment of zero-coordinated Na^0 in THF seen in Table 1 shows clearly that, in the absence of solvating THF oxygens, the ground-state wave function remains centered near the Na^+ core. However, the propertie of this uncoordinated Na^0 are clearly strongly perturbed from the gas phase. This is evident in Figure 5b, which shows that the ionization energy of the zero-coordinated Na^0 is 6.74 ± 0.06 eV, compared to the gas-phase value of 5.14 eV. This ~1.5 eV stabilization comes mainly from the long-range attractive polarization part of the THF pseudopotential. In addition to the larger ionization energy, the radius of gyration of zero-coordinated Na^0 in THF is significantly smaller than that of Na^0 in the gas phase. This can be understood as a result of Pauli repulsion from the first-solvation-shell THF molecules, which compresses the Na^0 electron density in the manner expected for what is essentially a particle trapped in a roughly spherical box. As the solvent coordination number increases, we see that the valence electron is progressively displaced from the Na^+ core, so that the neutral sodium species has an increasingly larger dipole moment. The driving force for this displacement of the electron density is the close proximity of the coordinating THF oxygen atoms, which are highly repulsive to the electron.[29] The radius of gyration of the electronic wave function also increases with coordination number as the electron becomes progressively less bound by the Na^+. By coordination number 6, the solvation shell around Na^+ is essentially complete and the valence electron occupies a solvent cavity adjacent to the primary Na^+ solvation shell. This species can thus be thought of as a solvated electron which is perturbed by the Coulombic influence of the solvent-separated Na^+; within the radiation chemistry community, this species is referred to as a sodium cation:solvated electron loose-contact pair (LCP; see Figure 6 for a representative MD snapshot of this species).

Having explored the changes in the ground state of Na^0 with increasing coordination by THF, we now turn to examine the changes in the properties of the electronic excited states, which are directly reflected in the Na^0 absorption spectrum. Figure 7 plots the absorption spectrum of Na^0 as a function of the THF-oxygen coordination number around the cation. For the zero-coordinated species (solid black curve), we see the absorption spectrum peaks at 2.5 eV, which is blue of the 2.14-eV gas-phase sodium D-line in our model.[28] This blue shift results from the compression of the ground- and excited-state wave functions (relative to the gas phase) due to the presence of the first solvation shell THF molecules. At higher coordination numbers, we see that the spectrum red shifts as the electron is displaced from the Na^+ core: the addition of each coordinating oxygen atom shifts the peak of the absorption spectrum by ~0.25 eV.

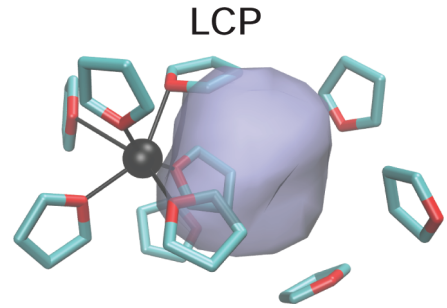

Figure 6. Molecular dynamics snapshot of a 6-fold coordinated neutral sodium species in THF, existing as a loose-contact pair (LCP), displayed in the same manner as Figure 2.

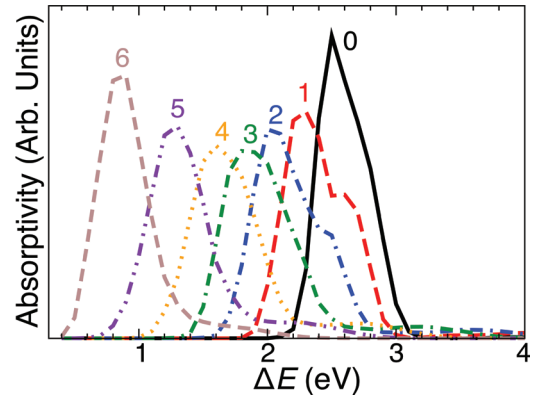

Figure 7. Calculated absorption spectra of the neutral sodium species in THF with different Na^+ coordination numbers (n_{Na^+} indicated by a number above each spectrum). The fact that each different coordination species is chemically and spectroscopically distinct has been verified in ultrafast transient hole burning experiments (ref 18).

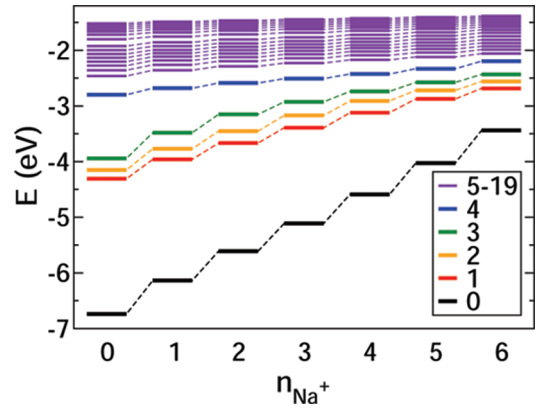

Figure 8. Mean electronic eigenvalues, E, as a function of Na^+ coordination number, n_{Na^+}. The lowest 20 eigenvalues at each coordination number are shown; the dashed lines connect them to guide the eye.

In addition to the red shift, we see that the spectrum broadens as n_{Na^+} is increased from 0 to 3, but then renarrows as n_{Na^+} is increased from 3 to 6. We also see that there is some structure in the spectrum (in the form of a shoulder on the blue edge) for $n_{Na^+} = 1$ and $n_{Na^+} = 2$ and that the blue tail only begins to develop when $n_{Na^+} \geq 2$.

We can understand these trends in the spectroscopy of Na^0/THF by considering how the electronic eigenvalues of Na^0 change with increasing solvent coordination of the Na^+ core. In Figure 8, we plot the lowest 20 ensemble-averaged eigenvalues of Na^0 (relative to the vacuum) as a function of the solvent coordination number; the dashed lines have been drawn between the energetically ordered eigenvalues at consecutive

coordination numbers to guide the eye (we do not discount the possibility that states may cross). The figure shows that the absorption spectrum of zero-coordinated Na^0 is composed of transitions from the ground state (black line) to the lowest three excited states (red, orange, and green lines), each of which corresponds to a 3s → 3p excitation. There is then a gap of ∼1 eV between state 3 and state 4 (blue line), which corresponds to a 4s-like state of sodium and therefore does not contribute to the absorption spectrum since it is dipole-forbidden from the ground state. The higher-lying states (5−19) of the zero-coordinated species are closely spaced and consist of a mixture of Rydberg-like states of the Na atom and solvent-supported cavity states that have also been seen in previous work to contribute to the high-energy spectral region of both the sodium anion[30] and the solvated electron in THF.[30,54,55]

As the solvent coordination number increases, Figure 8 shows that *all* of the electronic states of Na^0 are progressively destabilized as the electron is displaced from the Na^+ core, but the degree to which the different states are destabilized is not equal. The ground state, which overlaps the most with the Na^+ core, is destabilized to a greater extent than the excited states, explaining the red shift of the absorption spectrum with increasing coordination. Not surprisingly, the energetic locations of states 4−19, which contribute to the blue spectral tail in the absorption spectrum for $n_{Na^+} \geq 2$, are relatively insensitive to the coordination number. Finally, the way the width of the Na^0 absorption spectrum changes with coordination number can be explained by the energetic splitting of states 1−3, the low-lying *p*-like excited states. When only one or two THF oxygens coordinate the Na^+ core, the sodium atom experiences a highly asymmetric environment, with the solvent coordination predominantly destabilizing the highest *p*-like state more than the lower two, giving rise to the blue shoulder in the spectra of these low-coordinated species. This asymmetry reaches its maximum value when $n_{Na^+} = 3$, causing the three p states to be roughly evenly split, producing the maximum broadening of the spectrum. As the coordination number increases further, the electron starts to occupy its own solvent cavity, so that its solvation environment becomes more symmetric, causing the spectrum to narrow and the substructure to wash out.

We note that the idea of different solvent coordination numbers leading to distinct structure in the spectrum of Na^0 has experimental precedent. Piotrowiak and Miller measured the absorption spectrum of Na^0 in 2,5-dimethyltetrahydrofuran (2,5-DMTHF) and 2,2,5,5-tetramethyltetrahydrofuran (2,5-TMTHF),[2] two solvents that have dipole moments and dielectric constants similar to those of unmethylated THF. The presence of the methyl substituents at the α position, however, means that these solvent molecules are sterically hindered from tightly solvating alkali cations relative to the coordination that takes place in liquid THF. Indeed, Piotrowiak and Miller found that the absorption maximum of Na^0 in 2,5-DMTHF occurs at 1.69 eV (blue-shifted from that in THF by 0.25 eV) and that the spectrum contained a second peak at 2.15 eV.[2] The spectrum of Na^0 in 2,2,5,5-TMTHF was similar, but with three apparent peaks at 1.59, 1.72, and 2.17 eV. In light of our simulations, we assign the blue shift and spectral structure to the fact that Na^0 in these solvents has a lower average coordination number than in THF, consistent with the steric hindrance from the α-methyl groups.[56] And, as discussed further below, the spectra of Na^0 with different solvent coordination numbers recently have been observed experimentally using ultrafast transient hole-burning spectroscopy.[18]

3.4. Insights into the Pump−Probe Spectroscopy of Na^0/THF. In addition to providing a molecular-level interpretation of the steady-state absorption spectrum of Na^0 in THF and related solvents, our simulations also provide new insight into recent pump−probe experiments from both our laboratory[13,15] and others[16,17] that studied the equilibration dynamics of freshly created Na^0/THF. One set of these ultrafast transient absorption experiments examined the formation of Na^0/THF following photodetachment of an electron from sodide (Na^-).[13,16,17] These experiments observed that immediately[17] following removal of one of the two valence electrons from sodide, the neutral sodium atom that was left behind had an absorption spectrum whose peak is near that of the gas-phase sodium D-line. The spectrum then red-shifted on a ∼230 fs time scale, followed by an isosbestic interconversion on a ∼750 fs time scale and then a slow red shift on a ∼10 ps time scale to become the equilibrium sodium TCP spectrum.[13] The initial spectrum of Na^0 was interpreted as resulting from a sodium atom that, due to the large solvent cavity of its parent anion, weakly interacted with the solvent to yield a gas-phase-like absorption spectrum. The initial rapid red shift was attributed to solvation of the Na^0, which then underwent a chemical reaction to form the TCP, with the chemical interconversion giving rise to the isosbestic point. The nonequilibrium TCP was then observed to solvate on a ∼10 ps time scale.[13] Our simulations point to a new molecular interpretation of this otherwise generally correct experimental picture for these processes: the initial ∼230 fs red shift is the barrierless solvation of Na^0 to form the single-coordinated species, which then, because of a free energy barrier, undergoes a delayed "reaction" to form the two-coordinated species. The remaining ∼10 ps solvation time scale then corresponds to the reactions $n_{Na^+} = 2 \rightarrow 3 \rightarrow 4$. This assignment is supported by the fact that a 10 ps solvation time scale is too slow to ascribe to simple dielectric relaxation.[57,58] The relatively slow solvation observed is explained by the fact that 3-fold coordinated Na^0, which is formed from occasional fluctuations in our 1 ns equilibrium simulation, has a lifetime of several picoseconds (see Supporting Information). In an upcoming paper, we will present the full details of how relatively simple changes in solvent coordination number explain the full ultrafast transient spectroscopy of this system.[59]

Our assignment of the solvent coordination number as being the primary reaction coordinate in the solvation of Na^0/THF is also supported by a separate pump−probe study from our laboratory on the solvation dynamics of the (Na^+, e^-) TCP starting from the LCP.[15] In these experiments, electrons were photodetached from I^- and rapidly captured by nearby Na^+ counterions to form a population of sodium LCPs.[15] The initially created sodium cation:solvated electron LCPs were found to undergo a quasi-isosbestic interconversion to form a bluer-absorbing species, which then underwent a further spectral blue shift on a ∼5 ps time scale to produce equilibrium (Na^+, e^-) TCPs. Our simulations again provide a plausible molecular mechanism for the solvation dynamics of sodium TCPs that were created from LCPs: the quasi-isosbestic point corresponds to the reaction of the 6-fold coordinated LCPs to form 5-fold coordinated Na^0/THF species. The ∼5 ps blue shift then corresponds to the solvent coordination reaction $n_{Na^+} = 5 \rightarrow 4$.

Our group previously argued that the different solvation time scales for forming the equilibrium (Na^+, e^-) TCP starting from either photodetachment of sodide (∼10 ps) or electron attachment to Na^+ (∼5 ps) are indicative of a breakdown of the linear response (LR) approximation in describing the solvation dynamics of this system.[15] Our simulations provide a molecular

explanation for the different solvation time scales: starting from sodide, the solvation of Na^0 following its isosbestic interconversion involves overcoming two free energy barriers (for both $n_{Na^+} = 2 \rightarrow 3$ and $n_{Na^+} = 3 \rightarrow 4$), whereas the solvation of Na^0 following its isosbestic interconversion from the LCP involves the crossing of only one free energy barrier (between $n_{Na^+} = 5$ and 4). Thus, the apparent breakdown in the LR approximation can be seen as a direct result of the presence of free energy barriers along the reaction coordinate that describes the solvation of Na^0/THF.

The idea that the solvation dynamics of Na^0 are dictated by interconversions between spectroscopically distinct coordination numbers is further supported by recent pump−probe experiments from our group that measured the transient hole burning (THB) dynamics of Na^0/THF.[18] We found that after photoexciting Na^0/THF, the distribution of coordination numbers in the remaining ground-state population of Na^0 was modified from equilibrium. We argued that the spectral dynamics underlying the bleach recovery could be understood as interconversions between spectroscopically distinct species corresponding to different coordination numbers, with spectra that resemble those shown in Figure 7. Furthermore, the time scales of these interconversions match the time scales seen in the nonequilibrium pump−probe experiments that created Na^0 either via electron photodetachment of Na^-[13] or electron attachment to Na^+.[15,19] All of this suggests that no matter what the initial condition, the solvation dynamics of Na^0/THF are controlled by solvent motions that move the system over the free energy surface shown in Figure 4.

4. Conclusions

In this paper, we explored the equilibrium properties of a single sodium atom in liquid THF using mixed quantum/classical molecular dynamics simulation. We found that, in agreement with experimental interpretations,[1−4] the neutral sodium species in THF exists as a tight-contact pair in which the valence electron of sodium, on average, is displaced 1.43 ± 0.04 Å from the Na^+ core. As a result of this displacement, the 3s−3p gap of sodium is smaller in THF than in the gas phase. Moreover, the locally asymmetric solvent environment splits the 3p states, giving rise to a broad absorption spectrum peaked at ∼1.65 eV (1.43 eV experimental[4]). We found that the main driving force for displacement of the electron is the formation of a tight solvation shell of THF oxygens around the partially exposed Na^+ core of the atom. On average, four THF oxygens coordinate with Na^+; however, coordination numbers 3 and 5 are readily thermally accessible. The four-coordinated species predominates at equilibrium as a result of a balance between the solvation of Na^+, which favors high coordination numbers, and the costs of partially ionizing Na^0 and the energetic and entropic penalties to forming a highly ordered solvation shell around Na^+, which favor lower coordination numbers.

By using umbrella sampling to map out the free energy of Na^0/THF as a function of coordination number, we found that integer coordination numbers 1−6 correspond to local free energy minima, each separated by barriers of a few k_BT. This allows us to think about the different coordination numbers of Na^0/THF as chemically distinct species. Furthermore, each coordination species has a distinct electronic absorption spectrum that shifts from the visible to near-IR with increasing coordination number. The spectra of Na^0/THF species with different coordination numbers also have different shapes and widths, which is a direct consequence of the molecular details of the local solvent coordination. The idea that Na^0/THF's equilibrium absorption spectrum is composed of a number of spectroscopically distinct coordination numbers is also consistent with the transient hole burning spectroscopy of Na^0/THF.[18]

Finally, we were able to relate our findings to the results of recent pump−probe experiments that studied the solvation dynamics of Na^0/THF formed via both electron photodetachment of Na^- and electron attachment to Na^+.[13,15] In particular, the spectral dynamics of Na^0/THF during solvation can be interpreted in terms of dynamics on the free energy curve in the Na^+ coordination number reaction coordinate shown in Figure 4. The presence of free energy barriers along this reaction coordinate explains why slow solvation time scales (∼5−10 ps) were observed experimentally, and also why the linear response approximation was seen to break down for this system. In a forthcoming publication, we shall test this molecular-level interpretation of the solvation dynamics of Na^0/THF by using mixed quantum/classical molecular dynamics simulations to study the formation of a sodium TCP following electron detachment from Na^-/THF, affording a direct comparison between simulation and the experimental pump−probe spectroscopy.[59]

Acknowledgment. This work was supported by the National Science Foundation under Grant No. CHE-0908548 and the American Chemical Society Petroleum Research Fund under Grant No. 45988-AC,6. We also gratefully acknowledge the UCLA Institute for Digital Research and Education and the California NanoSystems Institute for allocating computer time for the calculations presented in this paper. We thank Molly Larsen and Art Bragg for insightful discussions and for a critical reading of this manuscript.

Supporting Information Available: Additional simulation details of how we constrain THF to be rigid and planar; molecular dynamics snapshots for all coordination numbers of the sodium TCP; a discussion of the equilibrium fluctuations in coordination number and the effects of density and temperature on the nature of the TCP. This material is available free of charge via the Internet at http://pubs.acs.org.

References and Notes

(1) Bockrath, B.; Dorfman, L. M. *J. Phys. Chem.* **1973**, *77*, 1002.
(2) Piotrowiak, P.; Miller, J. R. *J. Am. Chem. Soc.* **1991**, *113*, 5086–5087.
(3) Fletcher, J. W.; Seddon, W. A. *J. Phys. Chem.* **1975**, *79*, 3055–3064.
(4) Seddon, W. A.; Fletcher, J. W.; Sopchyshyn, F. C.; Selkirk, E. B. *Can. J. Chem.* **1979**, *57*, 1792–1800.
(5) Catterall, R.; Slater, J.; Symons, M. C. R. *Can. J. Chem.* **1977**, *55*, 1979–1986.
(6) Jou, F. Y.; Dorfman, L. M. *J. Chem. Phys.* **1973**, *58*, 4715–4723.
(7) Bar-Eli, K.; Tuttle, T. R. *J. Chem. Phys.* **1964**, *40*, 2508–2519.
(8) Sprik, M.; Impey, R. W.; Klein, M. L. *Phys. Rev. Lett.* **1986**, *56*, 2326–2329.
(9) Martyna, G. J.; Klein, M. L. *J. Chem. Phys.* **1992**, *96*, 7662–7671.
(10) Zurek, E.; Edwards, P. P.; Hoffmann, R. *Angew. Chem., Int. Ed.* **2009**, *48*, 8198–8232.
(11) Spezia, R.; Nicolas, C.; Archirel, P.; Boutin, A. *J. Chem. Phys.* **2004**, *120*, 5261–5268.
(12) Coudert, F.-X.; Archirel, P.; Boutin, A. *J. Phys. Chem. B* **2006**, *110*, 670–615.
(13) Cavanagh, M. C.; Larsen, R. E.; Schwartz, B. J. *J. Phys. Chem. A* **2007**, *111*, 5144–5157.
(14) Cavanagh, M. C.; Young, R. M.; Schwartz, B. J. *J. Chem. Phys.* **2008**, *129*, 134503.
(15) Bragg, A. E.; Cavanagh, M. C.; Schwartz, B. J. *Science* **2008**, *321*, 1817–1822.
(16) Shoshana, O.; Lustres, J. L. P.; Ernsting, N. P.; Ruhman, S. *Phys. Chem. Chem. Phys.* **2006**, *8*, 2599–2609.
(17) Shoshanim, O.; Ruhman, S. *J. Chem. Phys.* **2008**, *129*, 044502.

(18) Bragg, A. E.; Glover, W. J.; Schwartz, B. J. *Phys. Rev. Lett.* **2010**, *104*, 233005.
(19) Bragg, A. E.; Schwartz, B. J. *J. Phys. Chem. A* **2008**, *112*, 3530–3543.
(20) Tsoo, C. C.; Estrin, D. A.; Singer, S. J. *J. Chem. Phys.* **1990**, *93*, 7187–7200.
(21) Haug, K.; Metiu, H. *J. Chem. Phys.* **1991**, *95*, 5670–5680.
(22) Fois, E. S.; Gamba, A. *J. Chem. Phys.* **1994**, *100*, 9044–9049.
(23) Gross, M.; Spiegelmann, F. *J. Chem. Phys.* **1998**, *108*, 4148–4158.
(24) Bedard-Hearn, M. J.; Larsen, R. E.; Schwartz, B. J. *J. Phys. Chem. B* **2003**, *107*, 14464–14475.
(25) Chandrasekhar, J.; Jorgensen, W. L. *J. Chem. Phys.* **1982**, *77*, 5080–5089.
(26) Briggs, J. M.; Matsui, T.; Jorgensen, W. L. *J. Comput. Chem.* **1990**, *11*, 958–971.
(27) Phillips, J. C.; Kleinman, L. *Phys. Rev.* **1959**, *116*, 287.
(28) Glover, W. J.; Larsen, R. E.; Schwartz, B. J. *J. Chem. Phys.* **2008**, *129*, 164505.
(29) Smallwood, C. J.; Mejia, C. M.; Glover, W. J.; Larsen, R. E.; Schwartz, B. J. *J. Chem. Phys.* **2006**, *125*, 074103.
(30) Glover, W. J.; Larsen, R. E.; Schwartz, B. J. *J. Chem. Phys.* **2010**, *132*, 144102.
(31) Allen, M. P.; Tildesley, D. J. *Computer Simulation of Liquids*; Oxford University Press: London, U.K., 1992.
(32) Steinhauser, O. *Mol. Phys.* **1982**, *45*, 335.
(33) Hess, B.; Kutzner, C.; van der Spoel, D.; Lindahl, E. *J. Chem. Theory Comput.* **2008**, *4*, 435–447.
(34) Sorensen, D. C. *SIAM J. Matrix Anal. Appl.* **1992**, *13*, 357–385.
(35) Lehoucq, R. B.; Sorensen, D. C.; Yang, C. *ARPACK Users' Guide: Solution of Large-Scale Eigenvalue Problems with Implicitly Restarted Arnoldi Methods*; SIAM: Philadelphia, PA, 1998.
(36) For the equilibrium simulations described here, we verified that using a time step of 4 fs (as opposed to the 1 fs time step used in the nonequilibrium simulations of ref 24) was adequate to conserve the total system energy with root-mean-squared fluctuations of 0.55 meV. This improved energy conservation resulted from changing the method used to constrain the rigid THF molecules, as described in more detail in the Supporting Information.
(37) The ambient density of liquid THF predicted from the OPLS model is 0.8797 g cm^{-3},[26] which is sufficiently close to the experimental value that our use of the *NVT* ensemble at the experimental density is reasonable. Indeed, as we show in the Supporting Information, the results of our study are robust to modest changes in the simulation density.
(38) Andersen, H. C. *J. Comput. Phys.* **1983**, *52*, 24–34.
(39) Bussi, G.; Donadio, D.; Parrinello, M. *J. Chem. Phys.* **2006**, *126*, 014101.
(40) Webster, F.; Rossky, P. J.; Friesner, R. A. *Comput. Phys. Commun.* **1991**, *63*, 494–522.
(41) Minary, P.; Turi, L.; Rossky, P. J. *J. Chem. Phys.* **1999**, *110*, 10953–10962.
(42) Turi, L.; Hantal, G.; Rossky, P. J.; Boris, D. *J. Chem. Phys.* **2009**, *131*, 024119.
(43) Larsen, R. E.; Glover, W. J.; Schwartz, B. J. *Science* **2010**, *329*, 65–69.
(44) Sprik, M. *Faraday Discuss.* **1998**, *110*, 437–445.
(45) Grossfield, A. M. *WHAM version 2.0.2*, http://membrane.urmc.rochester.edu/Software/WHAM/WHAM.html (accessed Dec 12, 2009).
(46) Kumar, S.; Rosenberg, J. M.; Bouzida, D.; Swendsen, R. H.; Kollman, P. A. *J. Comput. Chem.* **1995**, *16*, 1339–1350.
(47) Using a higher density of histogram bins produced a free energy curve that was converged within the error bars.
(48) n_{Na^+} never fluctuated beyond 6.0, suggesting that a substantial free energy barrier exists for $n_{Na^+} > 6.0$, as would be expected from steric packing constraints.
(49) We note that the heights of the free-energy barriers shown in Figure 4 depend on our choice of the Fermi function width, κ. This is exemplified by the dashed green curve in Figure 4, which shows the free energy curve with $\kappa^{-1} = 0.1$ Å for windows $\eta = 2\ ^5/_6$ to $\eta = 4\ ^1/_6$. The dependence on κ results from the fact that n_{Na^+} is a nonlinear function of the particles' Cartesian coordinates, such that a logarithmic Jacobian term should be subtracted from A (see ref 44 and Khavrutskii, I. V.; Dzubiella, J.; McCammon, J. A. *J. Chem. Phys.* **2008**, *128*, 044106). Despite the dependence on κ, we believe that, given the low minimum in the RDF seen in Figure 3, the free energy barriers in Figure 4 are real.
(50) Although it is not clear whether the zero-coordinated species corresponds to a free energy local minimum, we include it in the analysis of the coordination species of Na^0 for completeness.
(51) Catterall, R.; Edwards, P. P. *J. Phys. Chem.* **1975**, *79*, 3010–3017.
(52) Seddon, W. A.; Fletcher, J. W.; Sopchyshyn, F. C.; Catterall, R. *Can. J. Chem.* **1977**, *55*, 3356–3363.
(53) Larsen, M. C.; McIlroy, S.; Schwartz, B. J.; Miller, J. R. Unpublished data.
(54) Bedard-Hearn, M. J.; Larsen, R. E.; Schwartz, B. J. *J. Chem. Phys.* **2005**, *122*, 134506.
(55) Bedard-Hearn, M. J.; Larsen, R. E.; Schwartz, B. J. *J. Chem. Phys.* **2006**, *125*, 194509.
(56) It is not clear whether the structure resolved in the experimental spectra of Na^0 in 2,5-DMTHF and 2,2,5,5-TMTHF (ref 2) results from a splitting of sodium's 3p states or from a distribution of coordination numbers at equilibrium. Transient hole burning spectroscopy would be one way to distinguish between these possibilities.
(57) Maroncelli, M. *J. Mol. Liq.* **1993**, *57*, 1–37.
(58) Chaudhari, A.; Khirade, P.; Singh, R.; Helambe, S. N.; Narain, N. K.; Mehrotra, S. C. *J. Mol. Liq.* **1999**, *82*, 245–253.
(59) Glover, W. J.; Larsen, R. E.; Schwartz, B. J. Manuscript in preparation.

JP103961J